Dynamics of Proton Transfer from Cation Radicals. Kinetic and Thermodynamic Acidities of Cation Radicals of NADH Analogues

Agnès Anne,[1a] Philippe Hapiot,[1a] Jacques Moiroux,[1a] Pedatsur Neta,[1b] and Jean-Michel Savéant*,[1a]

Contribution from the Laboratoire d'Electrochimie Moléculaire, Unité de Recherche Associée au CNRS No. 438, Université Paris 7, 2 Place Jussieu 75251 Paris Cedex 05, France, and Chemical Kinetics and Thermodynamics Division, National Institute of Standards and Technology, Gaithersburg, Maryland 20899. *Received October 21, 1991. Revised Manuscript Received February 3, 1992*

Abstract: Combined application of direct electrochemistry, redox catalysis, and laser flash photolysis has allowed the determination of the deprotonation rate constants of the cation radicals of four synthetic analogues of NADH by an extended series of bases. When sterically encumbered bases are avoided, the diffusion limit is reached in all cases at the upper edge of the driving force range. The intrinsic kinetic acidities, derived from the fitting of the rate data with a quadratic activation–driving force relationship, show no correlation with the thermodynamic acidities. They correlate with the homolytic bond dissociation energies of the $^{+\bullet}$C–H bond suggesting that the proton transfer from the cation radicals is better viewed as a concerted electron–H atom transfer rather than a stricto sensu proton transfer. Application of the dissociative electron-transfer theory shows that the homolytic bond dissociation energy is the main factor governing the reaction dynamics. Previous rate data from the literature pertaining to other cation radicals show the same trends.

Although investigated and discussed for many years,[2] the dynamics of proton transfer continue to raise considerable interest from both an experimental[3] and a theoretical point of view.[4] Deprotonation of organic cation radicals has attracted special attention in view of its relevance to the oxidation of organic compounds.[5] Analysis of the kinetics of proton transfer from this particular class of carbon acids may also provide valuable clues for a better understanding of the dynamics of proton transfer in general.

Chart I

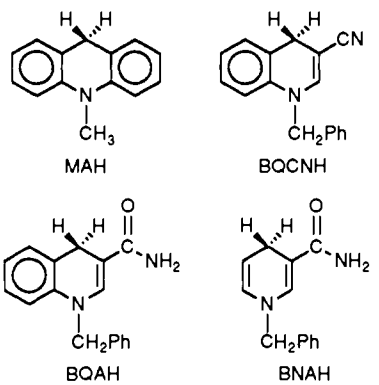

We have shown recently with the example of *N*-methylacridan that the comparative use of direct and indirect (redox catalysis) electrochemical techniques and of laser flash photolysis allows one to establish the mechanism of the oxidation of the substrate, AH, into A^+ and to measure the rate constants of the deprotonation of the $AH^{\bullet+}$ cation radical by adding bases up to the diffusion limit.[6a,b] Determination of the standard potentials, $E^0(AH^{\bullet+}+e^-/AH)$ and $E^0(A^++e^-/A^\bullet)$ by electrochemical techniques and of $E^0(A^++H^++2e^-/AH)$ by a slow equilibration spectrometric method[6c] will also allow the determination of the pK_a of the cation radical.

At 20 °C

$$0.058pK_a(AH^{\bullet+}/A^\bullet+H^+) = 2E^0(A^++H^++2e^-/AH) - E^0(AH^{\bullet+}+e^-/AH) - E^0(A^++e^-/A^\bullet) \quad (I)$$

(1) (a) Université de Paris 7. (b) NIST.

(2) (a) Eigen, M. *Angew. Chem. Int. Ed. Engl.* **1964**, *3*, 1. (b) Bell, R. P. *The Proton in Chemistry*, 2nd ed.; Cornell University Press: Ithaca, NY, 1973. (c) Caldin, E.; Gold, V., Eds. *Proton Transfer Reactions*; Chapman and Hall: London, 1975. (d) Marcus, R. A. *J. Phys. Chem.* **1968**, *72*, 891. (e) Cohen, A. O.; Marcus, R. A. *J. Phys. Chem.* **1968**, *72*, 4249. (f) Marcus, R. A. *Faraday Symp. Chem. Soc.* **1975**, *10*, 60. (g) Marcus, R. A. *Faraday Discuss. Chem. Soc.* **1982**, *74*, 7. (h) Albery, W. J. *Annu. Rev. Phys. Chem.* **1980**, *31*, 227. (i) Albery, W. J. *Faraday Discuss. Chem. Soc.* **1982**, *74*, 245. (j) Kresge, A. J. *Chem. Soc. Rev.* **1973**, *2*, 475. (k) Kresge, A. J. *Acc. Chem. Res.* **1975**, *8*, 354. (l) Kreevoy, M. M.; Konasewich, D. E. *Adv. Chem. Phys.* **1972**, *21*, 243. (m) Kreevoy, M. M.; Oh, S. W. *J. Am. Chem. Soc.* **1973**, *95*, 4805. (n) Hupe, D. J.; Wu, D. *J. Am. Chem. Soc.* **1977**, *99*, 7653. (o) Bernasconi, C. F. In *Techniques and Applications of Fast Reactions in Solution*; Gettins, W. J., Wyn-Jones, E., Eds.; Reidel: Dordrecht, 1979; pp 453–462. (p) Murdoch, J. R. *J. Am. Chem. Soc.* **1980**, *102*, 71. (q) Murdoch, J. R. *J. Am. Chem. Soc.* **1983**, *105*, 2660.

(3) (a) Mostly in nonprotic solvents,[3b,c] but see also refs, 3d and 3e. (b) Richtie, C. D.; Lu, S. *J. Am. Chem. Soc.* **1989**, *111*, 8542. (c) Richtie, C. D.; Lu, S. *J. Am. Chem. Soc.* **1990**, *112*, 7748. (d) Hibbert, F. *Adv. Phys. Org. Chem.* **1986**, *22*, 113. (e) Perrin, C. *Acc. Chem. Res.* **1989**, *22*, 268.

(4) (a) Phenomenological analysis of experimental activation vs driving force relationships,[4b-f] adaptation of Marcus equation to gas-phase proton transfer,[4g-i] and ab initio quantum mechanical modelling.[4j-n] (b) Jencks, W. P. *Chem. Rev.* **1985**, *85*, 511. (c) Murray, C. J.; Jencks, W. P. *J. Am. Chem. Soc.* **1990**, *112*, 1880. (d) Bunting, J. W.; Stefanidis, D. *J. Am. Chem. Soc.* **1988**, *110*, 4008. (e) Bunting, J. W.; Stefanidis, D. J. *J. Am. Chem. Soc.* **1989**, *111*, 5834. (f) Bunting, J. W.; Stefanidis, D. J. *J. Am. Chem. Soc.* **1990**, *112*, 779. (g) Jasinski, J. M.; Braumam, J. I. *J. Am. Chem. Soc.* **1980**, *102*, 2906. (h) Lim, K. F.; Brauman, J. I. *J. Chem. Phys.* **1991**, *94*, 7164. (i) Mest-Ner, M.; Smith, S. C. *J. Am. Chem. Soc.* **1991**, *113*, 862. (j) Scheiner, S. *Acc. Chem. Res.* **1985**, *18*, 174. (k) Cao, H. Z.; Allavena, M.; Tapia, O.; Eveleth, E. M. *J. Phys. Chem.* **1985**, *89*, 1581. (l) Gill, P. M. W.; Radom, L. *J. Am. Chem. Soc.* **1988**, *110*, 5311. (m) Swanton, D. J.; Marsden, D. C. J.; Radom, L. *Org. Mass Spectrom.* **1991**, *26*, 227. (n) Wolfe, S.; Hoz, S.; Kim, C. K.; Yong, K. *J. Am. Chem. Soc.* **1990**, *112*, 4186.

(5) (a) Schlesener, C. J.; Amatore, C.; Kochi, J. K. *J. Am. Chem. Soc.* **1984**, *106*, 7472. (b) Schlesener, C. J.; Amatore, C.; Kochi, J. K. *J. Phys. Chem.* **1986**, *90*, 3747. (c) Masnovi, J. M.; Sankararaman, S.; Kochi, J. K. *J. Am. Chem. Soc.* **1989**, *111*, 2263. (d) Manring, L. E.; Peters, K. S. *J. Am. Chem. Soc.* **1985**, *107*, 6452. (e) Dinnocenzo, J. P.; Banach, T. E. *J. Am. Chem. Soc.* **1989**, *111*, 8646. (f) Reitstöen, B.; Parker, V. D. *J. Am. Chem. Soc.* **1990**, *112*, 4968. (g) Parker, V. D.; Chao, Y.; Reitstöen, B. *J. Am. Chem. Soc.* **1991**, *113*, 2336.

(6) (a) Hapiot, P.; Moiroux, J.; Savéant, J-M. *J. Am. Chem. Soc.* **1990**, *112*, 1337. (b) Anne, A.; Hapiot, P.; Moiroux, J.; Neta, P.; Savéant, J-M. *J. Phys. Chem.* **1991**, *95*, 2370. (c) Anne, A.; Moiroux, J. *J. Org. Chem.* **1990**, *55*, 4608. (d) Andrieux, C. P.; Anne, A.; Moiroux, J.; Savéant, J. M. *J. Electroanal. Chem.* **1991**, *307*, 17.

(7) (a) Amatore, C.; Savéant, J-M. *J. Electroanal. Chem.* **1977**, *85*, 27. (b) Amatore, C.; Gareil, M.; Savéant, J-M. *J. Electroanal. Chem.* **1983**, *147*, 1. (c) Andrieux, C. P.; Savéant, J-M. Electrochemical Reactions. In Investigation of Rates and Mechanisms of Reactions. Bernasconi, C. P., Ed.; *Techniques of Chemistry*; Wiley-Interscience: New York, 1986; Vol. 6, Part 2, pp 305–310.

0002-7863/92/1514-4694$03.00/0

Table I. Deprotonation Rate Constants of the $AH^{\bullet+}$ Cation Radicals[a]

base	pK_a^{20}	log k, M^{-1} s^{-1}			
		MAH	BQCNH	BQAH	BNAH
2-fluoropyridine	4.2	3.3 ± 0.2[b]	6.2 ± 0.2[b]		
2-chloropyridine	6.3	4.2 ± 0.1[b]	7.0 ± 0.2[b]		
3-cyanopyridine	7.0	4.4 ± 0.2[b]	7.2 ± 0.2[b]		
4-cyanopyridine	8.0	4.8 ± 0.1[b]	7.5 ± 0.1[c]	6.9_5 ± 0.1[d]	7.3 ± 0.1[d]
3-chloropyridine	9.0	5.2 ± 0.2[b]		7.7 ± 0.1[d]	7.6_5 ± 0.1[d]
		5.3 ± 0.1[d]			
3-fluoropyridine	9.4	5.3 ± 0.2[b]	8.0 ± 0.1[c]	7.8 ± 0.1[c]	7.8 ± 0.1[c]
				7.9 ± 0.1[d]	7.8 ± 0.1[d]
nicotinamide	9.8			8.0 ± 0.1[d]	8.1 ± 0.1[d]
isonicotinamide	10.1				8.2 ± 0.2[c]
pyridine	12.3	6.5 ± 0.2[b]	8.6_5 ± 0.1[c]	8.6 ± 0.1[c]	8.9 ± 0.1[c]
		6.3 ± 0.1[c]		8.7_5 ± 0.1[d]	8.9 ± 0.1[d]
		6.6 ± 0.1[d]			
3-methylpyridine	13.5	6.3 ± 0.2[b]	8.9 ± 0.1[c]	8.9 ± 0.1[c]	9.0_5 ± 0.1[d]
		6.7_5 ± 0.1[d]		8.8 ± 0.1[d]	
3,5-dimethylpyridine	14.5	6.4 ± 0.2[b]	9.2 ± 0.1[c]	9.1 ± 0.1[c]	9.0_5 ± 0.1[c]
		6.9_5 ± 0.1[c]		8.9 ± 0.1[d]	8.9_5 ± 0.1[d]
		6.9_5 ± 0.1[d]			
ammonia	16.5	8.3 ± 0.2[d]			8.9 ± 0.1[d]
benzylamine	16.8	8.4 ± 0.1[c]			9.4 ± 0.1[c]
tert-butylamine	18.1	8.6 ± 0.1[c]		9.4 ± 0.1[c]	9.4 ± 0.1[d]
		8.4 ± 0.1[d]		9.8_5 ± 0.1[d]	
piperidine	18.9	8.9 ± 0.1[c]			
pyrrolidine	19.6	9.0 ± 0.2[c]			
1,3-diaminopropane[e]	19.7	8.7 ± 0.2[c]		9.7 ± 0.1[d]	9.7 ± 0.1[d]
		9.1 ± 0.1[d]			
1,4-diaminobutane[e]	20.1	9.5 ± 0.1[d]		9.9 ± 0.1[d]	9.8 ± 0.1[d]
acetate	22.3	10.1 ± 0.1[d]			10.0_5 ± 0.1[d]

[a] In acetonitrile at 20 °C. [b] Cyclic voltammetry at ultramicroelectrodes. [c] Redox catalysis. [d] Laser flash photolysis. [e] k values corrected for the statistical factor (2).

We applied these methods to obtain the rate constants of deprotonation of the cation radicals in acetonitrile of three analogues of NADH, BNAH, BQAH, and BQCNH (see Chart I) by an extended series of bases including pyridines and also aliphatic amines and acetate. Since the combination of methods described above allows the determination of the pK_a of each of the cation radicals in the series and since the pK_a of each base is known, it was possible to investigate, in each case, the variation of the activation energy with the exact driving force of the reaction. We could thus compare the intrinsic kinetic acidities, as derived from the intrinsic barriers (activation free energies at zero driving force), to the thermodynamic acidities. It was thus found that no correlation exists between these two quantities to the point that the cation radical that is thermodynamically the weakest acid is the fastest in terms of intrinsic kinetic acidity. We observed that, on the other hand, a good correlation exists between the intrinsic barrier and the homolytic bond dissociation energy ($AH^{\bullet+} \rightarrow A^+ + H^\bullet$) with a slope not far from one-fourth. A model viewing homolytic cleavage of the carbon–hydrogen bond of the cation radical, concerted with electron transfer, as the predominant reorganization factor in the reaction is suggested to account for these observations. It is shown to also fit literature kinetic data pertaining to other cation radicals.

Results

The rate constants for the deprotonation of the $AH^{\bullet+}$ cation radicals by a series of bases encompassing the largest possible range of pK_a's were obtained from the combined use of cyclic voltammetry at ultramicroelectrodes, redox catalysis, and laser flash photolysis. There is a lower limit of the pK_a's that can be investigated due to the basic properties of the starting AH molecules, leading to the reaction

$$AH^{\bullet+} + AH \rightarrow A^\bullet + AH_2^+ \quad (1)$$

Sound results are thus obtainable only when the reaction with the base is faster than the reaction with AH. Thus, even if the base was introduced in excess by a factor of about 1000, a limitation exists as to the possibility of investigating the deprotonation of the $AH^{\bullet+}$ cation radicals by weak bases. This is the reason that the lower pK_a limit was 4.2 with MAH and BQCNH but 8 for BQAH and BNAH. The latter compounds have indeed been observed to be more basic than the former.[6c]

Table II. Standard Potentials[a] and pK_a's[b]

	MAH	BQCNH	BQAH	BNAH
$E°(A^+H^+ + 2e^-/AH)$[c]	218 ± 24[6a]	257 ± 26[6c]	115 ± 25[6c]	22 ± 29[6c]
$E°(AH^{\bullet+} + e^-/AH)$	855 ± 4[d]	1144 ± 4[d]	924 ± 8[e]	786 ± 8[e]
$E°(A^+ + e^-/A^\bullet)$	−465 ± 10[d]	−520 ± 10[d]	−720 ± 10[d]	−1105 ± 10[d]
$pK_a(AH^{\bullet+}/A^\bullet + H^+)$[f]	0.8 ± 0.9[6a]	−1.9 ± 0.9	0.4 ± 0.9	4.7 ± 1.0

[a] In mV vs SCE. [b] In acetonitrile at 20 °C. [c] The main uncertainty occurs in the case of MAH.[6a] The other determinations are made by reference to MAH with a small additional error. The relative values in the series are thus known with a much better accuracy than the absolute values. The same is consequently true for the pK_a's. [d] Cyclic voltammetry at ultramicroelectrodes. [e] From the determination of k_{+e} by redox catalysis and k_{-e} by laser flash photolysis. [f] From eq 1.

Cyclic Voltammetry at Ultramicroelectrodes. Because of its limitations in the determination of the very high rate constants, the use of cyclic voltammetry at ultramicroelectrodes was restricted to MAH,[6a] in the pK_a range 4.2–14.5, and to BQCNH, in the range 4.2–7.0. For BQCNH, analysis of the current response as a function of the scan rate and substrate concentration led to the conclusion that the electrochemical oxidation follows the same DISP1 mechanism[7a,b] as observed before with MAH:[6a]

$$AH - e^- \rightleftarrows AH^{\bullet+} \quad (2)$$

$$AH^{\bullet+} + B \xrightarrow{k} A^\bullet + BH^+ \quad (3)$$

$$AH^{\bullet+} + A^\bullet \rightarrow A^+ + AH \quad (4)$$

The values of the deprotonation rate constant could thus be determined for the three weakest bases in the series (Table I) as well as the value of the standard potential of the $AH/AH^{\bullet+}$, $E^0(AH/AH^{\bullet+})$ (Table II).

As seen earlier (eq I), the standard potential of the $A^+/A^\bullet$ couple, $E^0(A^+/A^\bullet)$, is a useful quantity for estimating the pK_a of the $AH^{\bullet+}$ cation radical. Its values were derived from high scan rate cyclic voltammetry of the A^+ cations.[8]

(8) (a) See ref 8b for more details. (b) Anne, A.; Hapiot, P.; Moiroux, J.; Savéant, J-M. *J. Electroanal. Chem.*, in press.

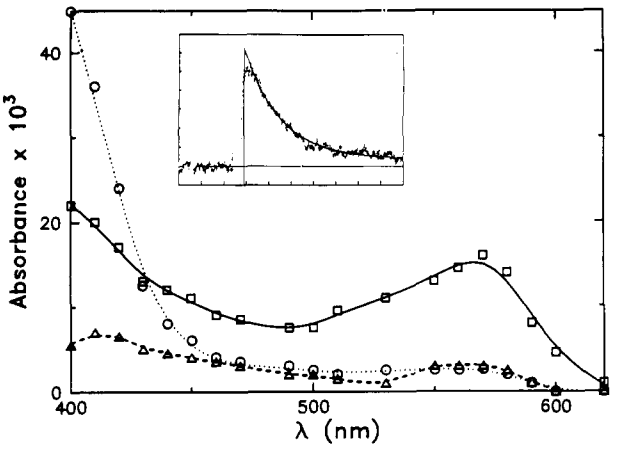

Figure 1. Transient absorption spectra recorded upon laser photolysis (351 nm) of an acetonitrile solution of BNAH (0.14 mM) and $CHBr_3$ (0.25 M) 1 μs (□) and 5 μs (○) after the pulse. After 400 μs the absorption at 500–600 nm decays to zero and that at <430 nm increases further. The lower (△) spectrum was recorded in the presence of 5 mM pyridine 1 μs after the pulse and shows the disappearance of the cation radical at 570 nm and possible formation of the neutral radical at 420 nm. The insert shows a typical trace at 570 nm; the time scale is 1 μs per division.

Laser Flash Photolysis. We have described recently[6b] how laser flash photolysis can be employed to achieve the one-electron oxidation of MAH into its cation radical in aerated acetonitrile containing carbon tetrachloride and to measure the rate constant of the deprotonation of $MAH^{\bullet+}$ by various bases. We have applied a similar method in the case of BQAH and BNAH.

The cation radicals of BQAH and BNAH have not been observed before. In the case of NADH in water, it has been shown[9] that $NADH^{\bullet+}$ can be obtained from a biphotonic reaction taking place at 351 nm. It exhibits a spectrum with two main bands at 370 and 550 nm and decays with a rate constant of 3.5×10^6 s^{-1}. Other authors[10a,b] attempted to photoxidize NADH and BNAH at 353 nm in the presence of various electron acceptors but did not observe the appearance of the corresponding cation radicals. With BQAH and BNAH in acetonitrile, we observed, upon irradiation by a 351-nm laser pulse, that little absorbance appears in the 550–650-nm region in the absence of electron acceptors other than oxygen. In the case of MAH, we have found earlier that the presence of 0.1% CCl_4 permits the formation of the $MAH^{\bullet+}$ radical in high yield.[6b] With BNAH, however, CCl_4 did not appear as an efficient quencher: even when CCl_4 was introduced in 10% volume, the absorbance around 570 nm remained very weak. By contrast, the replacement of CCl_4 by $CHBr_3$ allowed the production of $BNAH^{\bullet+}$ and $BQAH^{\bullet+}$ in good yield.

Figure 1 depicts the transient absorption spectra obtained upon laser flash irradiation of a mixture of BNAH and $CHBr_3$ in acetonitrile. The spectrum obtained 1 μs after the pulse exhibits a peak at 570 nm that we ascribed to $BNAH^{\bullet+}$ by analogy to the 550-nm peak of $NADH^{\bullet+}$.[9] After 5 μs most of this peak has decayed while a strong absorption appears in the 400–430-nm region. This absorption hampers the detection of the neutral radical, BNA•, which is known to slightly absorb around 420 nm.[11] As seen later on, this spectrum disappears upon addition of a base, suggesting that this spectrum is that of the protonated form of the starting material (AH_2^+) obtained upon deprotonation of the cation radical (reaction 1). This assignment was confirmed by the following set of pulse radiolysis experiments. HCl was generated by pulse radiolysis of a 1:1 CH_2Cl_2/CH_3CN mixture.[12] In the presence of BNAH a rapid rise of the absorbance in the 350–450-nm region is observed with a rate constant close to the diffusion limit (Figure 2). The $BNAH_2^+$ ion thus generated then decomposes during the next milliseconds. The occurrence of reaction 1 during the flash photolysis experiments where no exogeneous base was added is further confirmed by the observation that the lifetime of $BNAH^{\bullet+}$ decreases as the initial BNAH concentration is increased. A rate constant of $(3 \pm 1) \times 10^9$ M^{-1} s^{-1} for reaction 1 was estimated from the variation of the rate of decay of $BNAH^{\bullet+}$ with BNAH concentration.

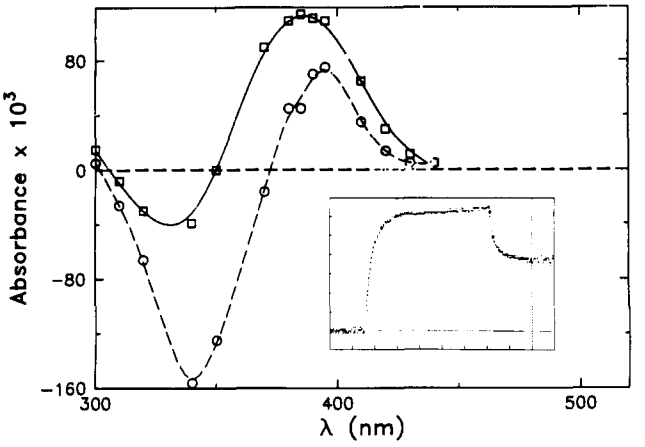

Figure 2. Transient differential absorption spectra recorded upon reaction of BNAH with HCl produced in the pulse radiolysis of CH_2Cl_2/CH_3CN (1:1), 10 μs (□) and 4 ms (○) after the pulse (BNAH, 0.14 mM). The insert shows a typical trace taken at 390 nm; the time scales in the three successive regions were 2 μs, 2 ms, and 100 ms per division.

We then investigated the rate constant of deprotonation of the $BNAH^{\bullet+}$ cation radical by a series of bases. The base was introduced in the solution in excess of 3–10 times and the rate of the deprotonation reaction was obtained from the decay of the 570-nm absorption band of $BNAH^{\bullet+}$. This method was preferred to the monitoring of the formation of the BNA• radical by means of its 420-nm band because of the weakness of this band and the fact that the radical subsequently disappears by reaction with the dioxygen present in the reaction medium. For each base concentration investigated the rate of protonation was observed to obey pseudo-first-order kinetics and the value of the second-order deprotonation rate constant, k, was derived from the slope of the linear plot of the first-order rate constant vs base concentration. Raising the concentration of $CHBr_3$ to 1.3 M has no effect on the k values thus determined. The values of k thus obtained are listed in Table I.

As discussed in the next section, the application of redox catalysis to the determination of the rate constant k rests on the measurement of the rate constant ratio k/k_{-e} where k_{-e} is the rate constant of back electron transfer between the mediator couple (Q/P) and the $AH^{\bullet+}/AH$ couple:

$$Q + AH \underset{k_{-e}}{\overset{k_{+e}}{\rightleftharpoons}} P + AH^{\bullet+} \qquad (2')$$

the standard potential of the mediator couple being negative to that of the $AH^{\bullet+}/AH$ couple. When the difference between the standard potentials is large, k_{-e} is likely to be close to the diffusion limit, k_{dif}. It is however useful to check this conclusion and to estimate the range of standard potential difference where it is valid. We used laser flash photolysis to obtain this piece of information. The rate constant k_{-e} of the reaction of $AH^{\bullet+}$ with the reduced form of the catalyst couple, P, was measured in the same way as its deprotonation by a base, simply substituting the base by P. The decay rate of $AH^{\bullet+}$ absorbance was found to linearly decrease upon raising the concentration of P (from 5×10^{-5} to 1.5×10^{-4} M). The rate constant k_{-e} was thus derived from the slope of the linear plot. The results are gathered in Table III.

The same procedures were applied to BQAH for determining k and k_{-e}. Figure 3 shows the transient absorption spectrum of $BQAH^{\bullet+}$ obtained 1 μs after irradiation of an aerated solution of BQAH in acetonitrile in the presence of $CHBr_3$ by a 351-nm

(9) Czochralska, B.; Linqvist, L. *Chem. Phys. Lett.* **1983**, *256*, 2597.
(10) Martens, F. M.; Verhoeven, J. W. *Recl. Trav. Chim. Pays Bas* **1981**, *100*, 228. (b) Martens, F. M.; Verhoeven, J. W.; Varma, C. A. G. O.; Bergwerp, P. *J. Photochem.* **1983**, *22*, 99.
(11) Land, E. J.; Swallow, A. J. *Biochim. Biophys. Acta* **1968**, *162*, 327.
(12) Levanon, H.; Neta, P. *Chem. Phys. Lett.* **1980**, *70*, 100.

Table III. Rate Constants and Driving Forces of the Reaction of $AH^{\bullet+}$ with Various Mediators

substrate	mediator (P)	$E°(Q+e^-/P)$, mV vs SCE	log k_{-e},[a] M^{-1} s^{-1}	$E°(AH^{\bullet+}+e^-/AH)$ – $E°(Q+e^-/P)$,[b] mV
MAH	bis(Pentamethylferrocene)	−101	10.0	956
	1,1′-dimethylferrocene	317	10.0	538
	n-butylferrocene	348	9.9	507
	ferrocene	405	9.9	450
	benzoylferrocene	655	9.5	200
BQCNH	promazine	756	10.0[c]	388
BQAH	bis(pentamethylferrocene)	−101	9.7	1025
	1,1′-dimethylferrocene	317	10.0	607
	n-butylferrocene	348	9.7	576
	ferrocene	405	9.8	519
	benzoylferrocene	655	9.1	269
BNAH	bis(pentamethylferrocene)	−101	10.0	886
	1,1′-dimethylferrocene	317	10.0	468
	n-butylferrocene	348	9.7	436
	ferrocene	405	9.8	381
	benzoylferrocene	655	9.7	130

[a] Determined by laser flash photolysis unless otherwise stated; the error is less than ±0.1. [b] $E°(AH^{\bullet+}+e^-/AH)$ from Table II. [c] From $E°(AH^{\bullet+}+e^-/AH)$ (Table II) and k_{+e} (Table IV).

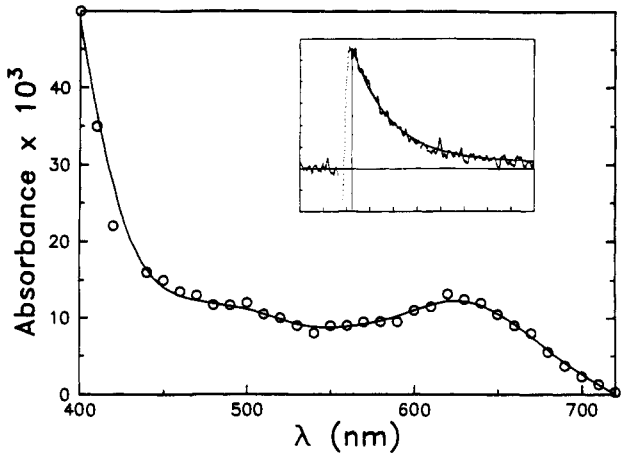

Figure 3. Transient absorption spectra recorded upon laser photolysis (351 nm) of an acetonitrile solution of BQAH (0.15 mM) and $CHBr_3$ (0.5 M) 1 μs after the pulse. The insert shows a typical trace at 620 nm; the time scale is 1 μs per division.

laser pulse. The system exhibits a maximum at 620 nm and decays rapidly giving rise to a strong absorption below 430 nm. The latter can be ascribed, by analogy with BNAH, to $BQAH_2^+$ produced by proton transfer from $BQAH^{\bullet+}$ to BQAH. The rate constant of this reaction was found to be $(1.5 \pm 0.5) \times 10^9$ M^{-1} s^{-1}. The rate constants of the reaction with bases (k) and with mediators (k_{-e}) listed in Tables I and III, respectively, were obtained from the decay of the 620-nm absorption band (Figure 3).

In the case of BQCNH, we observed that $CHBr_3$ is not efficient enough a quencher to generate the cation radical in a sufficiently short time. This falls in line with the fact that BQCNH itself is the most difficult to oxidize in the series (see Table V) and that the reducing powers of the excited states probably parallel those of the ground states. We did not pursue the search for a more efficient oxidative quencher since all the thermodynamic and kinetic quantities of interest could be determined through combined use of direct electrochemistry and redox catalysis (vide infra).

From the data in Table III we see that k_{-e} reaches the diffusion limit ($\log k_{-e} = \log k_{dif} = 9.9$, the k's being expressed in M^{-1} s^{-1}) as soon as the difference in standard potential, $E^0(AH^{\bullet+}+e/AH) - E^0(Q + e/P)$, is larger than 350 mV.

Redox Catalysis. We applied the redox catalysis method to the measurement of the deprotonation rate constant of the $BQCNH^{\bullet+}$, $BQAH^{\bullet+}$, and $BNAH^{\bullet+}$ cation radicals by an extended series of bases following procedures similar to those previously applied to the case of $MAH^{\bullet+}$.[6b]

Table IV. Mediators Used for the Redox Catalysis Determination of the Rate Constant of the Deprotonation Reaction 3 and Values of the Rate Constant of Forward Reaction 2′

substrate	mediator (P)	$E°(Q+e^-/P)$, mV vs SCE	log k_{+e}, M^{-1} s^{-1}
BQCNH	promazine	756	3.4
BQAH	4-nitrophenylferrocene	523	3.0
BNAH	*n*-butylferrocene	348	2.4
	ferrocene	405	3.4

The successive steps involved in the redox catalytic process are the following.

$$P \rightleftarrows Q + e^- \quad (5)$$

$$AH + Q \underset{k_{-e}}{\overset{k_{+e}}{\rightleftharpoons}} AH^{\bullet+} + P \quad (2')$$

$$AH^{\bullet+} + B \xrightarrow{k} A^{\bullet} + BH^+ \quad (3)$$

$$A^{\bullet} + Q \rightarrow A^+ + P \quad (6)$$

The oxidized form of the mediator couple, Q, is generated reversibly at the electrode from its reduced form which is introduced in the solution. The one-electron reversible cyclic voltammetric oxidation wave of P loses its reversibility and increases in height upon introduction of the substrate in the solution. The value of he ratio i_p/i_p^0 of the oxidation peak currents in the presence and absence of the substrate, respectively, is a reflection of the kinetics of the reactions following step 5. The mediators used in the present study (Table IV) were selected so that their standard potentials were close enough to that of the oxidation potential for a measurable increase of the current to be obtained and not too close so as to avoid overlapping of the catalytic and direct oxidation waves. In all cases, reaction 6 has a very large driving force, ranging from 1243 to 1510 mV (see Table II), and its rate constant is thus close to the diffusion limit. On the other hand, all $AH^{\bullet+}$ cation radicals are strong acids (Table II). It follows that reverse reaction 3 is much slower than reaction 6 and therefore that forward reaction 3 can be treated as an irreversible step. Under these conditions the kinetics of the set of reactions giving rise to the catalytic increase of the current are controlled by reaction 2′, a reversible up-hill reaction, and by reaction 3, which is irreversible. Two limiting situations are reached depending upon the value of $k_{-e}C_P/kC_B$ (C_P, concentration of mediator; C_B, concentration of base). In the cases we have investigated (Table I), the introduction of a base such as pyridine in large excess ($C_B/C_P > 50$) makes the ratio $k_{-e}C_P/kC_B$ sufficiently small for the kinetic control to be entirely by forward reaction 2′. The kinetics then exhibits a characteristic second-order behavior toward C_P and the value of k_{+e} can be derived from i_p/i_p^0 using the appropriate working curves.[6b,7c] The values of k_{+e} obtained in this manner are listed

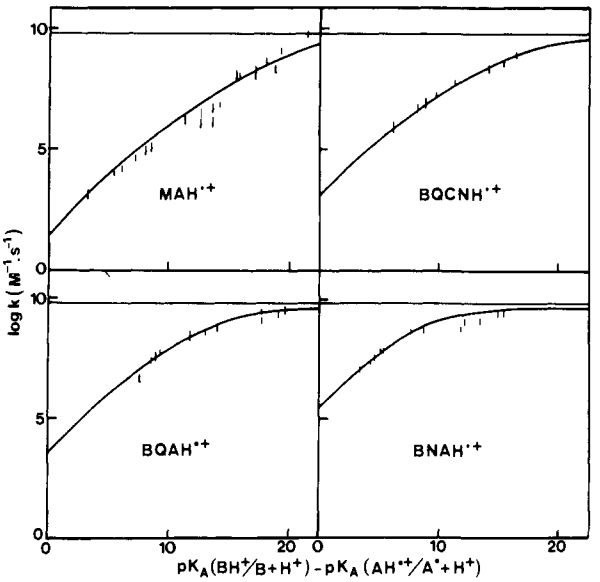

Figure 4. Variation of the deprotonation rate constant of the cation radicals, k, with the driving force of the reaction, $pK_a(BH^+/B+H^+) - pK_a(AH^{\bullet+}/A^{\bullet}+H^+)$.

in Table IV. Upon decreasing the concentration of base, the kinetic control tends to pass from forward reaction 2′ to reaction 3 (with (2′) acting as a preequilibrium). In the present study, the latter suitation was never reached owing to the fact that reaction 3 is fast, but the deviation from the former situation was large enough for reaching a mixed control behavior which allows, knowing k_{+e}, the determination of the ratio k_{-e}/k. The most precise results were obtained for a value of $C_P/C_{AH} = 0.5$. For the highest values of k, the concentration of base was decreased below the limit where reaction 3 can be regarded as pseudo-first order. We then used the working curves recently developed for these second-order conditions.[6d] Since the values of $E^0(AH^{\bullet+}+e^-/AH) - E^0(Q + e/P)$ were larger than 380 mV in all cases, we took log $k_{-e} = 9.9$ for deriving k from the measured values of the ratio k_{-e}/k.

The values of k thus obtained are listed in Table I. In the case of BQAH and BNAH, we used the values of k_{+e} derived from the redox catalysis experiments together with the values of k_{-e} obtained from laser flash photolysis (Table III, Figure 4) to compute the values of $E^0(AH^{\bullet+}+e^-/AH)$ (Table II), which in these two cases, unlike the cases of MAH and BQCNH, could not be reached by direct cyclic voltammetry.

Discussion

Figure 4 depicts the variation of the deprotonation rate constant, k, with the driving force of the reaction expressed as $pK_a(BH^+/B+H^+) - pK_a(AH^{\bullet+}/A^{\bullet}+H^+)$ for the four cation radicals.

One important observation is that, in all four cases, the deprotonation rate constant reaches the diffusion limit[13] as the driving force is made larger and larger. The driving force at which the diffusion limit is reached increases in the order BNAH < BQAH < BQCNH < MAH, which corresponds to the reverse order observed for the magnitude of the standard rate constant (rate constant at zero driving force). It must be emphasized in this connection that sterically encumbered bases have been purposely excluded from the correlation, particularly pyridines substituted in their ortho position(s) by alkyl groups.[14]

(13) The acetate ion gives a rate constant slightly larger than the value of log $k_{dif} = 9.9$ that we have derived from the laser flash investigation of the reaction between the reduced form of mediator and $AH^{\bullet+}$ described earlier. This may be explained by the fact that the reaction of $CH_3CO_2^-$ with $AH^{\bullet+}$ involves an attractive electrostatic work term.

(14) We have noted that *o*-methylpyridines tend to fall off the log k–driving force correlation in the case of $MAH^{\bullet+}$.[6a] We have recently extended these observations to other substituted pyridines in the framework of a systematic study of steric hindrance effects now in progress.

Table V. Kinetic and Thermodynamic Characteristics of the Cation Radicals

cation	$\Delta G^{\ddagger}_0$,[a,c] eV	$D(AH^{\bullet+}/A^+ + H^{\bullet})$,[b,c] eV	$pK_a(AH^{\bullet+}/A^{\bullet}+H^+)$[c] in CH_3CN	−gas basicity,[d] eV
$MAH^{\bullet+}$	$0.57_8 \pm 0.02$	1.80 ± 0.02	0.8 ± 0.03	8.55
$BQCNH^{\bullet+}$	$0.49_7 \pm 0.02$	1.59 ± 0.02	-1.9 ± 0.03	8.39
$BQAH^{\bullet+}$	$0.45_8 \pm 0.02$	1.52 ± 0.02	0.4 ± 0.04	8.52
$BNAH^{\bullet+}$	$0.37_3 \pm 0.02$	1.39 ± 0.02	4.7 ± 0.04	8.77

[a] From the fitting of the rate data as shown in figure 5. [b] Bond dissociation energy from the following thermodynamic cycle (free energies at 298 K): $AH^{\bullet+}_{CH_3CN} \leftrightarrow A^{\bullet}_{CH_3CN} + H^+_{CH_3CN}$ ($-0.059pK_a(AH^{\bullet+}/A^{\bullet}+H^+)$); $H^+_{CH_3CN} \leftrightarrow H^+_{H_2O}$ (−0.477[17a]); $A^{\bullet}_{CH_3CN} + H^+_{H_2O} \leftrightarrow A^+_{CH_3CN} + {}^1/_2H_{2,gas}$ [$E^0(A^+ + e^-/A^{\bullet})$ vs aqueous NHE = $E^0(A^+ + e^-/A^{\bullet})$ vs aqueous SCE − 0.242[17b] in V]; ${}^1/_2H_{2,gas} \leftrightarrow H^{\bullet}_{gas}$ (2.106[17a]). Thus: $\Delta G^0(AH^{\bullet+}/A^+ + H^{\bullet}) = 1.871 + 0.059pK_a(AH^{\bullet+}/A^{\bullet}+H^+) + E^0(A^+ + e^-/A^{\bullet})$ vs aqueous SCE and $D(AH^{\bullet+}/A^+ + H^{\bullet}) = 2.219 + 0.059pK_a(AH^{\bullet+}/A^{\bullet}+H^+) + E^0(A^+ + e^-/A^{\bullet})$ vs aqueous SCE (the entropies of formation of $AH^{\bullet+}$ and A^+ are practically the same and the entropy of formation of $H^{\bullet}_{gas}$ is 27.4 eu[17a]). [c] The values of the pK_a are taken from Table II and only the statistical error is indicated in this column and in the derivation of $\Delta G^{\ddagger}_0$ and $D(AH^{\bullet+}/A^{\bullet}+H^{\bullet})$. There is, in addition, a systematic uncertainty of ±0.08 on the pK_a as indicated in footnote *c* of Table II and therefore of ±25 meV on $\Delta G^{\ddagger}_0$ and of ±50 meV on $D(AH^{\bullet+}/A^+ + H^{\bullet})$. These uncertainties are however the same in magnitude and sign for all four compounds. [d] $\Delta G^0(AH^{\bullet+}_{gas}/A^{\bullet}+H^+) = 8.5 + 0.058pK_a(AH^{\bullet+}/A^{\bullet}+H^+)$. This approximate relationship was shown to be valid for several pyridines and other bases used in this study (see Table VI). Its applicability to the $AH^{\bullet+}$ cation radicals assumes that $\Delta G^0(AH^{\bullet+}_{CH_3CN}/AH^{\bullet+}_{gas}) - \Delta G^0(A^{\bullet}_{CH_3CN}/A^{\bullet}_{gas})$ is approximately the same as $\Delta G^0(BH^+_{CH_3CN}/BH^+_{gas}) - \Delta G^0(B_{CH_3CN}/B_{gas})$.

It is thus possible to fit the log k vs driving force experimental data by the following set of equations:

$$\frac{1}{k} = \frac{1}{k_{act}} + \frac{1}{k_{dif}}$$

$$k_{act} = Z \exp(-\Delta G^{\ddagger}/RT)$$

(k_{act} and k_{dif}, activation and diffusion controlled bimolecular rate constants, respectively; Z, collision frequency; $\Delta G^{\ddagger}$, activation barrier free energy) and, using a quadratic Marcus-type activation–driving force relationship,

$$\Delta G^{\ddagger} = (\Delta G^{\ddagger}_0 + W_R)\left[1 + \frac{\Delta G^0 - W_R + W_P}{4\Delta G^{\ddagger}_0}\right]^2 \quad \text{(II)}$$

($\Delta G^{\ddagger}_0$, intrinsic barrier free energy; in eV, $\Delta G^0 = 0.058pK_a(AH^{\bullet+}/A^{\bullet}+H^+) - pK_a(BH^+/B+H^+)$; W_R and W_P, work required for the formation of the precursor and successor complexes, respectively, from reactants at infinite distance).

The fact that the diffusion limit is reached at high driving forces indicates that W_R is small as expected from the fact that there is no electrostatic charge interactions between the reactants. We thus neglected W_R in the following analyses. We also, for the same reason, neglected W_P. A quite satisfactory fit of the experimental data is obtained in this way (Figure 4).[16] It should be noted in this connection that, as is generally the case with homogeneous

(15) (a) Although the Marcus model[2f] leading to eq II is strictly speaking applicable only to outer-sphere electron-transfer reactions, it has been empirically applied in many instances to reactions in the course of which bonds are broken and/or formed (see ref 15b and references cited therein, particularly proton-transfer reactions).[2,4] (b) Savéant, J-M. *Adv. Phys. Org. Chem.* **1990**, *26*, 1.

(16) (a) For Z, the bimolecular collision frequency derived from the Smoluchovski equation, we took an average of 3×10^{11} M^{-1} s^{-1}.[16b] The values of k_{act} thus obtained were multiplied by 2 to take account of the fact that deprotonation of $AH^{\bullet+}$ may involve one or the other of the two hydrogen atoms borne by the functional carbon (para to the nitrogen). (b) Kojima, H.; Bard, A. J. *J. Am. Chem. Soc.* **1975**, *97*, 6317.

(17) (a) Nicholas, A. M. P.; Arnold, D. R. *Can. J. Chem.* **1982**, *60*, 2165. (b) *Handbook of Chemistry and Physics*, 52th ed.; CRC Press: Cleveland, OH, 1971; p D111.

Table VI. Thermodynamic Characteristics of the Bases

base	pK_a[a]	−GB,[b] eV	−GB − 0.058pK_a, eV	IP,[c] eV	$D(BH^+/B^{\bullet+}+H^\bullet)$,[d] eV
2-fluoropyridine	4.2	8.85	8.60	10.07	5.66
2-chloropyridine	6.3	8.98	8.61	9.91	5.66
4-cyanopyridine	8.0	8.80	8.33	9.95	5.14
3-fluoropyridine	9.4	8.98	8.42	9.79	5.15
pyridine	12.3	9.22	8.49	9.30	4.90
3-methylpyridine	13.5	9.33	8.53	9.04	4.75
ammonia	16.5	8.52	7.54	10.20	5.10
benzylamine	16.8	9.17	8.17	8.85	4.40
tert-butylamine	18.1	9.24	8.16	8.50	4.15
piperidine	18.9	9.42	8.30	7.85	3.75
pyrrolidine	19.6	9.38	8.22	8.20	3.95
			av ≈8.5		

[a] In acetonitrile from ref 20. [b] GB gas basicity from ref 21. [c] Adiabatic ionization potential from ref 21. [d] Homolytic bond dissociation energy from $D(BH^+/B^{\bullet+}+H^\bullet) = -GB + IP - 13.971$ as results from the appropriate thermodynamic cycle and the H^+,$H^\bullet$ thermodynamic data contained in ref 17a.

rate data,[15b] the precision does not really allow the quadratic character of the Marcus eq II to be experimentally tested. What is remarkable, however, is that the values of the intrinsic barrier, $\Delta G^{\ddagger}_0$ resulting from the fitting procedure (Table V), accord with the average values of the symmetry factor, $\alpha = \partial\Delta G^{\ddagger}/\partial\Delta G^0$, that can be derived from the approximate fitting of the data by a straight line. The average values of α thus derived, ranging between 0.3 and 0.35, are indeed clearly below 0.5, the predicted value at $\Delta G^0 = 0$ (when $W_R = W_P = 0$), in accord with

$$\alpha = 0.5\left[1 + \frac{\Delta G^0 - W_R + W_P}{4\Delta G^{\ddagger}_0}\right]$$

The values of $\Delta G^{\ddagger}_0$ thus obtained[16] (Table V) are a measure of the *intrinsic* kinetic acidities of the $AH^{\bullet+}$ cation radicals (the lower $\Delta G^{\ddagger}_0$, the larger the intrinsic kinetic acidity). An initial observation is that the intrinsic barriers are large unlike the case of "normal" acids. It is also worthy of notice that a single Brønsted plot is obtained in each case in spite of the fact that bases from quite different families were opposed to the cation radicals. This observation points to the notion that the dynamics of the deprotonation reaction is mainly governed by reorganization factors pertaining to the cation radicals rather than to the opposing bases.

There are two ways of explaining the dissociation of the carbon–hydrogen bond in the present cation radicals or of the bond between carbon or other atoms and hydrogen in other acids: one is homolytic (transfer of a H atom) and the other is heterolytic (transfer of a proton). In the gas phase the homolytic dissociation energy of the cation radicals ($^{+\bullet}CH \rightarrow {}^+C + H^\bullet$) is considerably smaller than their heterolytic dissociation energy ($^{+\bullet}CH \rightarrow {}^\bullet C + H^+$) (Table V). For "normal" acids such as the acid forms of the bases used in this study, the homolytic dissociation energy ($BH^+ \rightarrow B^{\bullet+} + H^\bullet$) is also smaller than their heterolytic dissociation energy ($BH^+ \rightarrow B + H^+$) but to a much lesser extent (Table VI).

In addition to this, at the ground-state carbon–hydrogen distance, covalent-type structures

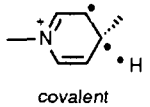

covalent

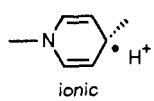

ionic

are likely to have considerably larger weights than ionic-type structures in terms of valence bond description of the cation radicals. The opposite is true for "normal" acids (or a least the covalent and ionic structures have comparable weights). We are thus led to the schematic picture of the potential-energy curves in the gas phase sketched in Figure 5.

With "normal" acids, the passage from the gas phase to a polar solvent results in a dramatic lowering of the proton energy leading to the conclusion that the heterolytic cleavage is certainly favored

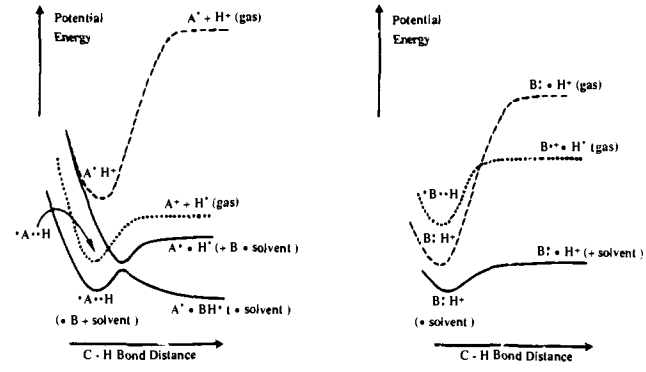

Figure 5. Schematic picture of the potential energy curves.

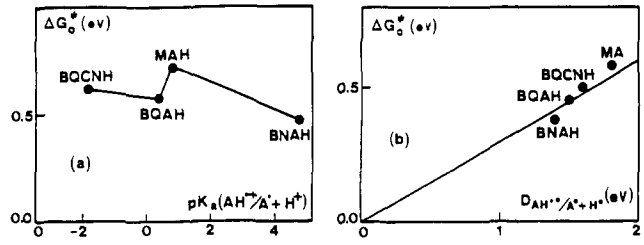

Figure 6. Plot of the variation of the intrinsic barrier, $\Delta G^{\ddagger}_0$ (opposite to the intrinsic kinetic acidity), of the deprotonation of the $AH^{\bullet+}$ cation radical with pK_a (a) and with homolytic bond dissociation energy, $AH^{\bullet+} \rightarrow A^+ + H^\bullet$ (b).

as compared to the homolytic cleavage and that the latter requires small energies as sketched in the right-hand side of Figure 5. Combining this type of dissociation potential energy curve with a curve of the same type representing the opposing acid–base couple will result in a small activation intrinsic barrier, possibly so small that diffusion control will prevail. If this is not the case, i.e., if activation control still prevails, the activation barrier should be related to the pK_a of the acid: the lower the pK_a, the smaller the intrinsic barrier.

That the present cation radicals do not fall in this category is clearly seen in Figure 6a. Not only are the intrinsic bariers large (of the order of 0.5 eV), but they do not increase with the pK_a. On the other hand, the less acidic cation radical, $BNAH^{\bullet+}$, is the fastest to deprotonate and the most acidic cation radical, $BQCNH^{\bullet+}$, is the second slowest just after $MAH^{\bullet+}$. More generally, if a trend is to be found in the correlation between intrinsic barrier and pK_a, it is the opposite of what is expected: the smaller the pK_a, the slower the deprotonation.

In the case depicted on the left-hand side of Figure 5, the passage from the gas phase to a polar solvent containing the opposing base has no dramatic effect on the homolytic dissociation curve. There is a slight decrease of both the bottom and the plateau of the Morse curve with negligible variation of their difference since $AH^{\bullet+}$ and A^+ have the same charge and closely similar sizes. On the other hand, a considerable change occurs in the heterolytic dissociation curve under the influence of the opposing base and the solvent. It thus practically becomes repulsive for all carbon–hydrogen distances. We are thus led to the following reaction pathway (Figure 5): The reaction starts with the stretching of the C–H bond in a homolytic fashion along a potential energy curve that can be approximated by the homolytic dissociation Morse curve of the $AH^{\bullet+}$ cation radical. Inside the solvent cage, the stretching of the C–H bond in the homolytic mode is energetically much more favorable than in the heterolytic mode. However, as the C–H bond distance increases, the approach of the base and of solvent molecules stabilizes more and more H^+ and therefore favors the heterolytic dissociation. The dissociative potential energy curve of the latter then crosses the homolytic Morse curve and the reaction thus occurs with a transition state located at the (avoided) crossing of the two curves.

It is thus expected that the intrinsic barrier be correlated with the homolytic bond dissociation energy: the smaller the homolytic

bond dissociation energy, the smaller the intrinsic barrier. As seen in Figure 6b, such a correlation indeed appears in the experimental data.

According to this reaction pathway, the reaction appears as a *concerted transfer of an electron and of a H atom* rather than a *stricto sensu* proton transfer. Thus the theory previously developed for dissociative electron transfer and experimentally illustrated by the heterogeneous and homogeneous reductive cleavage of alkyl halides,[18] should also be applicable in the present case. It predicts that the activation–driving force relationship obeys eq II and that the contribution of the bond cleavage to the intrinsic barrier is one-fourth of the homolytic bond dissociation energy. The correlation shown in Figure 6b has a slope of 0.3, only slightly larger than the theoretical slope of 0.25. Homolytic cleavage of the $^{\bullet+}$C–H bond thus appears to be the dominant factor governing the dynamics of proton transfer in the series of cation radicals investigated in the present study.

It should be emphasized that the main reason that the present cation radicals do not behave as "normal" acids, but that their deprotonation rather involves a concerted transfer of an electron and a H atom, is that their charge is delocalized from the departing proton, being mostly borne by the nitrogen atom in the covalent structure above.

It is interesting to note that the same observations appear to apply to another series of cation radicals for which extensive deprotonation rate data are available, namely the polymethylbenzene cation radicals (hexamethyl, pentamethyl, and 1,2,4,5- and 1,2,3,4-tetramethyl).[5a,b] The intrinsic barrier is practically the same for all four compounds ($\Delta G^{\ddagger}_0$ = 0.67 eV[19]) and so is the homolytic bond dissociation energy ($D(AH^{\bullet+}/A^{+}+H^{\bullet})$ = 2.35 eV[19]), while the pK_a of the $AH^{\bullet+}$ varies from 1 to −2 in the series. Thus, in this case too, the intrinsic kinetic acidity does not parallel the thermodynamic acidity but rather the homolytic bond dissociation energy. The ratio of $\Delta G^{\ddagger}_0$ over $D(AH^{\bullet+}/A^{+}+H^{\bullet})$ is 0.29, i.e., very close to the value found in the present study.

The model developed above implies that formation and/or breaking of the B–H bond do not interfere to a large extent in the dynamics of the reaction. In the nitrogen and oxygen acids corresponding to the bases used in the present study, B: H^+ ionic structures are expected to predominate over $^{+}B{\bullet\bullet}H$ covalent structures in the ground state and bond breaking is likely to be heterolytic in polar solvents, i.e.: $BH^+ \rightarrow B: + H^+$ (as seen in Table VI, in the gas phase, the homolytic bond dissociation energy is still smaller than the heterolytic bond dissociation energy, but to a much lesser extent than with $AH^{\bullet+}$ cation radicals). In other words, these acids are expected to behave as "normal acids".

The cross reaction

$$^{+}AH^{\bullet} + B \rightarrow A^{\bullet} + {}^{+}HB$$

would thus involve three concerted steps: homolytic cleavage of the C–H bond, electron transfer, and heterolytic formation of the H–B bond. That $\Delta G^{\ddagger}_0$ is somewhat larger than $0.25D(AH^{\bullet+}/A^{+}+H^{\bullet})$, as noted earlier, may thus correspond to a small contribution of the B–H^+ bond-breaking/bond-formation to the activation barrier. This contribution is however certainly small for the following reasons. If we allowed for such a contribution to the intrinsic barrier, this would be dependent on the strength of the BH^+ (the stronger the acid, the smaller the contribution). $\Delta G^{\ddagger}_0$ in eq II would then depend upon ΔG^0 which would result in a change of the symmetry factor $\alpha = \partial\Delta G^{\ddagger}/\partial\Delta G^0$. As noted before there is a good consistency between the value of $\Delta G^{\ddagger}_0$ and that of α when fitting the rate data with eq II without allowing the intrinsic barrier to vary with ΔG^0, thus implying that the contribution of BH^+ stretching to the dynamics of the reaction is small. The fact that the B–H bond cleavage and formation do not interfere to a large extent in the dynamics of the reaction is thus related to an easy dissociation of BH^+ under the influence of solvent molecules, resulting in a transition-state structure in which the B–H distance would be much larger than the C–H distance. Another factor that could very well contribute to the activation barrier is solvent reorganization. For outersphere electron transfers between molecules of similar sizes in similar solvents, the contribution of solvent reorganization of the intrinsic barrier is of the order of 0.1 eV.[15b,16b] Taking account of this effect would result in a better accord with the predictions of the dissociative electron-transfer model developed above.

Experimental Section

Instrumentation, procedures, and materials were the same as previously described,[6,22] the excimer laser utilizing XeF for 351 nm with a pulse duration of 20–40 ns and pulse energies of ca. 100 mJ.[23] The *p*-nitrophenylferrocene mediator was prepared by treatment of ferrocene with *p*-nitrobenzenediazonium tetrafluoroborate in acetone[24] and purified by chromatography on neutral alumina with dichloroethane as the eluent, followed by crystallization from a dichloroethane/cyclohexane mixture. Mp 173 °C. Anal. Calcd for $C_{16}H_{23}NO_2Fe$: C, 62.57; H, 4.27; N, 4.56. Found: C, 62.47; H, 4.26; N, 4.72.

Conclusions

The combined use of direct electrochemistry, redox catalysis, and laser flash photolysis has permitted measurement of rate constants for the deprotonation of the cation radicals of MAH, BQCNH, BQAH, and BNAH by an extended series of bases. Avoiding the use of sterically encumbered bases, the diffusion limit was reached in all four cases at the higher edge of the driving force range. The rate data were satisfactorily fitted by a simple quadratic Marcus-type equation resulting in a good consistency between the value of the intrinsic barrier and that of the average symmetry factor. The intrinsic kinetic acidity thus measured by the value of the intrinsic barrier shows no correlation with the thermodynamic acidity measured by the pK_a of the cation radicals. On the contrary, the intrinsic barriers are correlated with the homolytic bond dissociation energy of the $^{+\bullet}$C–H bond. Proton transfer from this series of cation radicals thus appears as a concerted electron–H atom transfer rather than a *stricto sensu* proton tranfer.[25] The same conclusion also applies to the data reported in the literature concerning the deprotonation of other cation radicals. Application of the dissociative electron-transfer theory to these deprotonation reactions shows that the reaction

(18) Savéant, J-M. *J. Am. Chem. Soc.* **1987**, *109*, 6788.

(19) The intrinsic barrier free energies of deprotonation of the methylbenzene cation radicals were derived from the rate data[5b] in exactly the same manner as in the present study: sterically encumbered bases, including 2,6-dimethylpyridine, were excluded from the fitting of the experimental data to eq II. The work terms W_R and W_P were neglected, the collision frequency was taken as equal to 3×10^{11} M^{-1} s^{-1}, and the statistical factors (18 for hexamethylbenzene, 15 for pentamethylbenzene, 12 for 1,3,4,6- and 1,2,5,4-tetramethylbenzene) were taken into account. In these conditions, $\Delta G^{\ddagger}_0$ was found to be practically the same for all four compounds, $\Delta G^{\ddagger}_0$ = 0.67 eV. The pK_a's in acetonitrile are 1, −1, −2, and −2, respectively.[5b] The standard potentials $E^0(A^{+}+e^{-}/A^{\bullet})$ were known for the benzyl (0.97 V vs NHE), the 4-methylbenzyl (0.75 V vs NHE), and the 3-methylbenzyl (0.94 V vs NHE) radicals.[19b] From these data, the standard potentials for the four polymethylbenzyl radicals investigated can be estimated in an incremental fashion to be 0.25 (pentamethylbenzyl), 0.47 (tetramethylbenzyl), and 0.50 (2,4,5- and 2,3,4-trimethylbenzyl). It follows (footnote *b* in Table V) that $D(AH^{\bullet+}/A^{+}+H^{\bullet})$ is approximately the same in the series, being equal to 2.35 eV in average leading to $\Delta G^{\ddagger}_0/D(AH^{\bullet+}/A^{+}+H^{\bullet})$ = 0.29. (b) Sim, B. A.; Milne, P. H.; Griller, D.; Wayner, D. D. *J. Am. Chem. Soc.* **1990**, *112*, 6635.

(20) (a) The pK_a's of the pyridinium cations in acetonitrile are from ref 20b. Those of nicotinamide and isonicotinamide were deduced from a correlation of the pK_a value in water[20c] with that in acetonitrile. The other pK_a's are from ref 20c. (b) Cauquis, G.; Deronzier, A.; Serve, D.; Vieil, E. *J. Electroanal. Chem.* **1975**, *60*, 205. (c) *Handbook of Biochemistry*, 2nd ed.; Sober, H. A. Ed.; CRC Press: Cleveland, OH, 1973; p J216. (d) Kolthoff, I. M.; Chantoni, M. K.; Bhownik, S. *J. Am. Chem. Soc.* **1968**, *90*, 23. (e) Coetzee, J. F. *Prog. Phys. Org. Chem.* **1967**, *4*, 76.

(21) Aue, D. H.; Bowers, M. T. Stabilities of positive ions from equilibrium gas-phase basicity measurements. In *Gas Phase Ion Chemistry*; Bowers, M. T., Ed.; Academic Press: New York, 1969; Vol. 2, Chapter 9, p 1.

(22) The identification of commercial equipment or material does not imply recognition or endorsement by the National Institute of Standards and Technology, nor does it imply that the material or equipment identified are necessarily the best available for the purpose.

(23) Huie, R. E.; Clifton, C. L. *Int. J. Chem. Kinet.* **1989**, *21*, 611.

(24) Beckwith, A. L. J.; Leydon, R. J. *Aust. J. Chem.* **1966**, *19*, 139.

(25) (a) During the reviewing of the present paper, an elegant picosecond study of proton transfer from phenol cation radical in ammonia clusters appeared which confirms the validity of our approach and conclusions.[25b] The potential energy curves used to rationalized the data are indeed of exactly the same type as those pictured in Figure 5. (b) Steadman, J.; Syage, J. A. *J. Am. Chem. Soc.* **1991**, *113*, 6786.

dynamics are predominantly governed by the homolytic dissociation energy of the $^{+\bullet}C-H$ bond, although other factors such as solvent reorganization should be taken into account to a minor extent.

Acknowledgment. This work has been jointly supported by the CNRS, the Office of Basic Energy Sciences of the US Department of Energy. P.H. thanks the NIST for allowing him to carry out the laser flash photolysis experiments and Dr. R. E. Huie for his help in using the laser system.

Registry No. MAH radical cation, 105784-79-0; BQCNH radical cation, 141063-18-5; BQAH radical cation, 141063-19-6; BNAH radical cation, 72533-28-9; NADH radical cation, 88764-56-1.

One-Electron-Reduction Potentials of Pyrimidine Bases, Nucleosides, and Nucleotides in Aqueous Solution. Consequences for DNA Redox Chemistry[1]

S. Steenken,* J. P. Telo,[2] H. M. Novais,[2] and L. P. Candeias

Contribution from the Max-Planck-Institut für Strahlenchemie, D-4330 Mülheim, Germany.
Received November 18, 1991

Abstract: The reduction potentials in aqueous solution of the pyrimidine bases, nucleosides, and nucleotides of uracil (U) and thymine (T) were determined using the technique of pulse radiolysis with time-resolved spectrophotometric detection. The electron adducts of U and T were found to undergo reversible electron exchange with a series of ring-substituted *N*-methylpyridinium cations with known reduction potential. From the concentrations of the pyrimidine electron adducts and the reduced *N*-methylpyridinium compounds at electron-transfer equilibrium, the thermodynamical equilibrium constants were obtained and from these the reduction potentials. The results show U and T and their nucleosides and nucleotides to have very similar reduction potentials, ~ -1.1 V/NHE at pH 8, i.e., the effect of methylation at C5, C6, or of substitution at N1 is small, ≤ 0.1 V. In the case of cytosine (C) the electron adduct is protonated (probably at N3), even up to pH 13. The protonated adduct ($C(H)^{\bullet}$) undergoes a reversible electron transfer with the *N*-methylpyridinium cations. This is accompanied in one direction by transfer of a proton but by that of a water molecule in the other direction. As a result of the protonation of the electron adduct, the effective ease of reduction of C in aqueous solution is similar to that of U and T. It is suggested that in DNA the tendency for $C^{\bullet-}$ to be protonated (by its complementary base G) is larger by ≥ 10 orders of magnitude than that for protonation of $T^{\bullet-}$ by its complementary base A. This results in C and not T being the most easily reduced base in DNA. A further consequence is that lack of neutralization by *intra*pair proton transfer of $T^{\bullet-}$ enables the irreversible *extra*-pair protonation on C6 of the radical anion to take place.

Introduction

The destructive, mutagenic, and carcinogenic effect of ionizing radiation on living matter is almost exclusively due to the changes induced in the DNA of the cell nucleus.[3] If is for this reason that there has been a continuing and, lately, increasing interest to unravel the chains of mechanism by which the oxidizing and the reducing species that result from ionization of a molecule lead to the biologically visible damage.[4] On a molecular or "chemical" level one of the questions that has attracted considerable attention is whether the lesions to the pyrimidine and purine bases, which are produced in a *statistical* way, lead to damage at *specific* sites. Evidence for such "damage migration" phenomena has originally come from ESR studies in matrices at low temperatures,[4] but the conclusions[4] have recently been supported by methods such as pulse radiolysis[5,6] or laser photolysis[7] on DNA (bases) in aqueous solution at room temperature. There have also been theoretical studies on the feasibility of charge or energy transduction between bases of different nature or along the DNA chain.[8] The ESR evidence available to data can be summarized[4] by stating that, at room temperature, the negative charge produced in the ionization is trapped by thymine and the positive one by guanine. This is equivalent to saying that thymine is the most electron-affinic and guanine the most easily oxidized base under "DNA conditions", i.e., as constituents of the polynucleotide chain of DNA. This result has been regarded as being in agreement with the electron affinities (EA) and the ionization potentials (IP) of the bases. Concerning the *ionization potentials*, experimentally determined values are available,[9] and these show the purines to be more easily oxidized than the pyrimidines, and, among the former, guanine to be the best electron donor of all the bases, and this is in agreement with the results[10] of MO calculations.

(1) A preliminary report on this topic was given at the International Radiation Biology Conference held at New Orleans, LA, April 1990.

(2) Instituto Superior Tecnico, P-1096 Lisboa, Portugal.

(3) For reviews see, e.g.: (a) *Effects of Ionizing Radiation on DNA*; Bertinchamps, A. J., Hüttermann, J., Köhnlein, W., Teoule, R., Eds.; Springer: Berlin, 1978. (b) *Mechanisms of DNA Damage and Repair*; Simic, M. G., Upton, A. C., Eds.; Plenum: New York, 1986. (c) von Sonntag, C. *The Chemical Basis of Radiation Biology*; Taylor and Francis: London, 1987.

(4) For reviews see, e.g.: (a) Reference 3a. (b) Bernhard, W. A. *Adv. Radiat. Biol.* **1981**, *9*, 199. (c) Hüttermann, J. *Ultramicroscopy* **1982**, *10*, 25. (d) Symons, M. C. R. *J. Chem. Soc., Faraday Trans. 1* **1987**, *83*, 1. (e) Close, D. M.; Nelson, W. H.; Sagstuen, E. In *Electronic Magnetic Resonance of the Solid State*; Weil, J. A., Ed.; Canadian Society of Chemistry: Ottawa, Canada, 1987; p 237. (f) Hüttermann, J. In *Radical Ionic Systems*; Lund, A., Shiotani, M., Eds.; Kluwer: Dordrecht, 1991; pp 435-62. (g) Bernhard, W. A. Initial Sites of One Electron Attachment in DNA. In *The Early Effects of Radiation on DNA*; Fielden, E. M., O'Neill, P., Eds.; Nato ARW Series, Springer: 1991; Vol. H **54**, pp 141-54.

(5) Sevilla, M. D.; Failor, R.; Clark, C.; Holroyd, R. A.; Pettei, M. *J. Phys. Chem.* **1976**, *80*, 353.

(6) Visscher, K. J.; Hom, M.; Loman, H.; Spoelder, H. J. W.; Verberne, J. B. *Radiat. Phys. Chem.* **1988**, *32*, 465.

(7) Candeias, L. P.; Jones, G. D. D.; O'Neill, P.; Steenken, S. *Int. J. Radiat. Biol.* **1992**, *61*, 15.

(8) Gueron, M.; Eisinger, J.; Shulman, R. G. *J. Chem. Phys.* **1967**, *47*, 4077. Voltz, R. *Radiat. Res. Rev.* **1968**, *1*, 301. Dee, D.; Baur, M. E. *J. Chem. Phys.* **1974**, *60*, 541.

(9) (a) Hush, N. S.; Cheung, A. S. *Chem. Phys. Lett.* **1975**, *34*, 11. (b) Peng, S.; Padva, A.; LeBreton, P. R. *Proc. Natl. Acad. Sci. U.S.A.* **1976**, *73*, 2966. (c) McGlynn, S. P.; Dougherty, D.; Mathers, T.; Abdulner, S. In *Excited States in Organic Chemistry and Biochemistry*; Pullman, B., Goldblum, N., Eds.; Reidel: Dordrecht, 1977; p 247.

0002-7863/92/1514-4701$03.00/0